Modeling and Simulation of Transient Winds in Downbursts/Hurricanes

Lijuan Wang, Ahsan Kareem

NatHaz Modeling Laboratory, University of Notre Dame, Notre Dame, Indiana, USA

ABSTRACT

The non-stationarity and localization of energetics in the transient wind fields have posed difficulty in proper modeling and simulation of these events. Utilizing recent developments in time-frequency analysis framework, i.e., the wavelet and Hilbert transforms and empirical mode decomposition, this paper seeks to highlight the evolutionary features of these wind fields by offering schemes for their modeling and simulation. With the help of time-frequency analysis tools, hurricane winds are characterized as a summation of time-varying mean and fluctuating components. A simulation approach based on a time-frequency framework is proposed for generating winds at different locations during the passage of a downburst. Numerical examples are presented to demonstrate the efficiency and effectiveness of the proposed modeling and simulation schemes.

KEYWORDS: Downburst; Hurricane; Non-stationary processes; Wavelet transform; Hilbert transform; Instantaneous frequency

INTRODUCTION

Extreme winds experienced in hurricanes and thunderstorms are of significant concern to structural engineers since these winds are responsible for their damaging effects on buildings and structures. Rapid variations in wind speed and direction observed in downburst and hurricane winds underscores the non-stationary features of these wind fields. The non-stationary wind time histories are characterized not only by time-varying mean speeds but also by time-dependent power spectra. In recognition of the significance of capturing these features in predicting the structural response and attendant performance-based design (Yeh and Wen 1990; Conte and Peng 1992), the limitations of traditional stationary wind model have been examined (Ashcroft 1994). Autoregressive models have been attempted to model non-stationary wind data collected in the field (Smith and Mehta 1993). Gurley and Kareem (1999) applied wavelet transforms to analyse wind time histories and identified response characteristics dependent on higher response modes when the turbulent structure of the wind changes in time through wavelet transform. Recently, Chen and Xu (2004), Wang and Kareem (2004^a) analyzed typhoon-induced non-stationary wind speed by modeling it as a deterministic time-varying mean wind speed component plus a zero mean stationary fluctuating wind speed component. The empirical mode decomposition and wavelet transform were utilized to extract time-dependent mean. This paper assesses the efficacy of extracting the time varying mean wind speed by the two different approaches, i.e., discrete wavelet decomposition and empirical mode decomposition. With the re-definition of turbulence wind characteristics, the wind speed data recorded during Hurricane Lili, 2002 was analyzed. The results are then compared to those obtained through traditional approach based on assumption of stationary wind model.

The second part of the study focuses on the simulation of downburst winds. Whereas current wind loading codes and wind engineering tests rely exclusively on boundary layer wind profiles. Field observations made during the Northern Illinois Meteorological Research on Downburst (NIMROD) project (Fujita 1985) and the Joint Airport Weather Studies (JAWS) project (McCarthy *et al.* 1982) have revealed that downburst winds possess significantly different velocity profiles which have a maxima close to the ground with lower velocities in the upper part of the outflow layer of cold air. A number of efforts have been made in the literature to model and simulate thunderstorm downburst winds to study associated wind loads on structures. Holmes (2000) proposed an empirical model of the horizontal wind speed and direction in a traveling downburst, based on the impinging jet model by the vector summation of translation speed and the radial wind speed induced by an impinging jet. However, the variations of wind speed with height is not incorporated in this model, which has been accounted by several other researchers. Oseguera and Bowles (1988) have proposed a vertical profile expression satisfying the requirements of fluid mass continuity, without consideration of the storm movement. Vicroy (1992) has developed an axisymmetric, steady-state empirical model for the vertical profile which is a modified version of the Oseguera/Bowles' model. Wood *et al.* (2001) have advanced a generic empirical equation to predict the normalized mean velocity profile based on downdraft wind tunnel experimental data, which showed reasonable agreement with a simplified CFD analysis. More recently, Chen and Letchford (2004) have proposed a hybrid model, in which the mean wind speed is modeled combining both Wood's (2001) vertical velocity profile and Holmes' (2000) empirical model for horizontal wind speed, and the fluctuations in velocity are modeled as a uniformly modulated evolutionary vector stochastic process.

In most of the aforementioned efforts for numerical modeling and simulation of downburst winds, the variation of wind speed in space (height/radial distance) is described in the profile shape function; however, the actual time dependence of the evolutionary behavior of the wind field is fully not considered. The detection of non-stationary structure embedded in downburst wind would make it possible to capture localized pattern in the flow field. Chen and Letchford (2005) applied proper orthogonal decomposition to the time-varying means, standard deviations and normalized fluctuations for modeling and numerically simulating downbursts. Wang and Kareem (2004[a]) utilized a wavelet based time-frequency framework to model flow field in transient flows like eyewall of hurricanes and downburts. This paper seeks to highlight the evolutionary characteristics of downburst in time-frequency framework, involving the wavelet and Hilbert transforms. A stochastic simulation model is proposed to generate downburst wind field based on recorded downburst wind data. Example simulations are presented to demonstrate the effectiveness of the proposed time-frequency approach to simulate downburst wind flows.

THEORETICAL BACKGROUND

The classical Fourier transform (FT) approach has been a popular tool in the field of signal processing for decades due to its strength to present the power spectrum of a signal, however, the intrinsic global sinusoidal decomposition limits its application to stationary processes. The short-time Fourier transform (STFT) overcomes this limitation by involving a moving-window which permits application of FT to non-stationary signals. Yet the fixed window width involved in the STFT dictates a constant resolution in time-frequency domain and impedes its ability to detect highly localized components. Alternatively, the wavelet transform (WT) provides an attractive venue in which non-stationary signals can be characterized in the time-frequency domain. The WT in tandem with Hilbert transform (HT) will be used in this study to extract valuable evolutionary information from the hurricane/downburst wind data and subsequently used for simulation of these wind fields.

WAVELET TRANSFORM

Generally, WT falls in two categories: continuous wavelet transform (CWT) and discrete wavelet transform (DWT). CWT uses discretely sampled data, but the shifting process is smoothly carried out across the sample length with a flexibility in the selection of scale (frequency) resolution. On the other hand, DWT has orthogonal basis and is broken into dyadic blocks which entails shifting and scaling based on a power of 2. The dilation function of DWT can be viewed as a tree of low and high pass filtering operations followed by sub-sampling by 2 which successively decomposes a signal like a dyadic filter bank. Through a set of basis functions, the dilation and translation of the parent wavelet function, the WT provides a bank of wavelet coefficients representing a measure of similitude between the basis function and the signal at time t and scale a (Kareem and Kijewski, 2002), as shown below:

$$W_x(a,t) = \frac{1}{\sqrt{a}} \int_{-\infty}^{\infty} X(t)\phi^*(\frac{t-\tau}{a})dt \tag{1}$$

The discrete version of it is expressed as

$$W_x(i,j) = \sum_n X(n)\psi_{i,j}(n) \tag{2}$$

where $\psi_{i,j}(n)$, the wavelet function, is given by

$$\psi_{i,j}(n) = 2^{i/2}\psi(2^i n - j) \tag{3}$$

The localized wavelet coefficients represents the energy at corresponding time intervals of the signal. The visualization of the squared wavelet coefficients on time-scale domain is referred to as scalogram, which reveals time-varying energy over frequency. To identify correlation between signals, the squared coefficients are replaced with the product of the wavelet coefficients of two different processes, which provides a view of the coincident events between the processes, revealing time-varying pockets of correlation over frequency (Gurley and Kareem 1999). Besides offering a multi-resolution decomposition, the time-frequency character of WT allows adaptation of both traditional time and frequency domain system identification approaches to examine nonlinear and non-stationary data (Kijewski and Kareem 2003). The classical DWT does not exhibit the desirable property of shift-invariance, i.e., in general the DWT of a translated signal is not the translated version of the DWT of the signal. As a special version of the DWT, the stationary wavelet transform (SWT) does not include the sub-sampling step, thus ensuring the desirable property of translation invariance. For additional details, reference should be made to Percival and Walden (2000).

HILBERT TRANSFORM

The time-frequency contents of a signal can be tracked by way of instantaneous frequency of the signal encapsulated in the analytic signal format, which is a function of time varying amplitude and phase and can be obtained by the HT of the signal as expressed by:

$$H(t) = \frac{1}{\pi} P \int \frac{X(\tau)}{t-\tau} d\tau \tag{4}$$

in which τ is a time variable and P denotes the Cauchy Principle Value. The sum of the random variable and its HT, which are complex conjugate pair, results in an analytic signal, which can be equally expressed in an exponential form:

$$\hat{X}(t) = X(t) + iH(t) = a(t)e^{i\theta(t)} \tag{5}$$

where $a(t)$ and $\theta(t)$ denote the instantaneous amplitude and instantaneous phase of $X(t)$, respectively. The instantaneous frequency is defined as the time-varying derivative of the instantaneous phase of the analytic signal:

$$\omega(t) = \frac{d\theta(t)}{dt} \tag{6}$$

The HT cannot inherently accommodate signals with multiple frequency components thus requiring that multicomponent signals be transformed into mono-component signals prior to the implementation of the HT. Huang *et al.* (1998) introduced an empirical mode decomposition (EMD) to decompose data into a finite number of "intrinsic mode functions (IMF)". They preferred this approach over the filtering offered by the WT to obtain a narrow band signal as they believed that wavelet based filtering may contaminate the data by spurious harmonics caused by non-linearity and non-stationarity of data. Recently, the efficacy of EMD and WT based analysis has been highlighted in Kijewski-Correa and Kareem (2004). Also, Olhede and Walden (2004) have shown that the SWT-based projection produces mono-component separation that admits well-behaved Hilbert transform with results superior to those obtained by the empirical mode decomposition, even for sinusoids that theoretically contain intrinsic mode functions. This study utilizes SWT in the proposed simulation algorithm and decomposes a possibly multi-component non-stationary process into the summation of mono-component processes:

$$X(t) = \sum_{n=1}^{N} D_n(t) + A(t) \tag{7}$$

in which n represents the level of decomposition; $D_n(t)$ denotes the detail function at level n and $A(t)$ is the approximation function, which represents the trend of $X(t)$.

NON-STATIONARY WIND MODEL

In the analysis of wind effects on structures, traditionally, the longitudinal wind speed is assumed to be a stationary random process, which can be expressed as

$$U(t) = \overline{U} + u(t) \tag{8}$$

in which $\overline{U}$ is a constant mean wind speed, $u(t)$ is a longitudinal fluctuating wind speed component. The constant mean wind speed denotes an average over a time interval T, which is usually taken as one hour. In this study, the non-stationary wind speed is modeled as the sum of a deterministic time-varying wind speed and a zero-mean stationary random process as fluctuating component:

$$U(t) = \overline{U}(t) + u'(t) \tag{9}$$

where $\overline{U}(t)$ is the temporal trend of wind speed and $u'(t)$ is the fluctuating component which can be taken as a zero-mean stationary process (Wang and Kareem 2004[a]). After a time-varying mean wind speed $\overline{U}(t)$ has been identified, the fluctuating wind speed $u'(t)$ can be acquired by subtracting the time-varying mean wind speed $\overline{U}(t)$ from the measured wind speed time history, $u'(t) = U(t) - \overline{U}(t)$. As the fluctuating wind speed $u'(t)$ is assumed to be a zero-mean stationary process, the standard deviation and the probability density distribution and the wind spectrum of the fluctuating component can be obtained by replacing $u(t)$ by $u'(t)$ in the traditional definition of these quantities.

For non-stationary wind speed time history with time-dependent mean, the turbulence intensity of non-stationary wind speed is proposed to be given by the expected value of the time-dependent turbulence intensity over the time interval T.

$$I_{u',T} = E[\frac{\sigma_{u',T}}{\overline{U}_T(t)}] \tag{10}$$

in which $E[\,]$ denotes the expected value over the time interval T; $\sigma_{u',T}$ represents the standard deviation of the fluctuating wind speed over the time interval T. Accordingly, the gust factor is defined as the maximum ratio of time-varying mean wind speed over time t_1 to the corresponding hourly time-varying mean wind speed:

$$G(t_1) = max[\frac{\overline{U}_{t_1}(t)}{\overline{U}_{3600}(t)}] \tag{11}$$

in which t_1 is normally equal or less than 3600s. The integral length scale in the direction of the flow is defined as

$$L_{u'} = \overline{U}(t)\int_0^\infty \frac{R_{u'}(\tau)}{\sigma_{u'}^2}d\tau = \frac{\overline{U}(t)}{4\sigma_{u'}^2}S_{u'}(0) \tag{12}$$

where $R_{u'}(\tau)$ denotes the autocorrelation function of $u'(t)$, and $S_{u'}$ represents its Fourier transform. Utilizing the calculated length scale of longitudinal wind speed fluctuations, the commonly used von Karman spectrum is recast as:

$$\frac{nS_{u'}(n)}{\sigma_{u'}^2} = \frac{4nL_{u'}/\overline{U}(t)}{[1+70.8(nL_{u'}/\overline{U}(t))^2]^{5/6}} \tag{13}$$

The following section deals with data analysis involving wavelets and EMD to capture the time varying mean wind.

DATA ANALYSIS

DISCRETE WAVELET DECOMPOSITION

The set of hurricane data analyzed in this section was measured during Hurricane Lili, 2002 by the University of Florida researchers (Gurley 2002). As shown in Fig. 1, nineteen consecutive hours of data was sampled at 1/3 Hz. Fig. 2(a) demonstrates the 5 levels of signal sub-components and residue of the signal decomposed by DWT at 10 levels. From the figure, it is obvious that as the level number increases, the frequency component decreases and the residue matches the trend of the corresponding time-averaged mean quite well. Figs. 2(b) demonstrates the comparison of constant hourly mean and the time varying hourly mean of the 11^{st} hour of the signal, in which the time-varying means were obtained by DWT. Obviously, the approximation reflects the trend of the signal, while the hourly mean remains constant during the hour. Correspondingly, the fluctuating process is the original signal minus hourly mean, or the approximation in the case of DWT. Probability density functions of the corresponding fluctuating process derived from the constant mean, and 600s-mean of the 15^{th} hour data are shown in Figs. 2(c) together with the fitted Gaussian function to the data. It can be noted that the pdf derived from the constant mean deviates from the Gaussian, while that from the time-varying mean exhibits a better match with the Gaussian. It has been noted that often hurricane winds have been perceived as non-Gaussian by examining the pdf without any prior conditioning of the data. Nonetheless, this observation may still be valid in strong convective regions of a hurricane.

For the calculation of the integral length scale (Eq. 12), the low frequency component of $S_{u'}(n)$ is sensitive to different time-averaged means, which influences the calculated value of the length scale. As the low frequency component increases in the time varying mean, the value of $S_{u'}(0)$ decreases, resulting in smaller integral scale. Using hourly mean, 1200s-mean, 600s-mean, 300s-mean, and 150s-mean, corresponding calculated length scales are 94m, 90m, 85m, 79m and 70m, respectively. Figs. 2(d) shows the power spectral density functions of the two fluctuating processes of the 18^{th} hour data using hourly mean given by DWT, together with a fitted von Karman spectrum. It is observed that the fluctuating component derived from the time-varying mean has lower energy at low frequencies than the corresponding process with a constant mean. This can be explained as the very low frequency components have already been filtered out of the fluctuating component. At high frequencies, there is no discernible difference. The von Karman spectrum was fitted using the respective value of the length scale. Using proposed Eqs. (10) and (11), wind characteristics such as turbulence intensity and gust factor are reported in Figs. 2(e) and 2(f), along with the traditional approach. It is observed in Fig. 2(f) that by using 1200s time-varying mean, the turbulence intensity is very similar to that given by the constant mean, with slightly reduced values. Gust factors obtained by the time-varying mean have a similar trend in comparison with the traditional method.

EMPIRICAL MODE DECOMPOSITION

The empirical mode decomposition was utilized to obtain the time-varying mean of the wind speed data. Fig. 3(a) shows some of the IMFs of the signal in which the bottom plot shows the residue, which gives the trend of the original signal. In this study, the residue was taken as the corresponding time-varying mean. Results are shown with the residue as time varying mean in Fig. 3(b). It can be noted that the time-dependent mean matches the trend of the signal. The pdf is shown in Fig. 3(c), and the power spectral density function is presented in Fig. 3(d) using 600s-mean, together with the corresponding von Karman spectrum. Using hourly mean, 600s-mean, and 150s-mean, corresponding turbulence length scales were found to be 96m, 90m, and 85m, respectively. Using Eq. 10 and Eq. 11, the turbulence intensity and gust factor were obtained. The results are compared to the traditional method in Figs. 3(e) and 3(f). It is observed that the gust factors and the turbulence intensity have trend similar to those of the traditional method with some exception.

SIMULATION

A host of methods for numerical simulation of non-stationary processes based on one sample process have been developed over the years. Initially, by utilizing prescribed evolutionary spectrum, stochastic models including parametric time series (Deodatis and Shinozuka 1988) and stochastic decomposition models (Li and Kareem 1991) have been proposed to simulate earthquake ground motions and produced satisfactory results. The difficulty of applying those models to measured signals lies in the fact that the envelop functions utilized in the procedures are predetermined, regardless of the time-varying frequency component embedded in actual records. This neglect of non-stationarity in frequency has certainly brought mathematical convenience, however, studies have found that the temporal variation of the frequency component can have a significant effect on the response of structures (Yeh and Wen 1990; Conte 1992). Progress in the estimation of time dependent spectra of non-stationary progresses (Scherer *et al.* 1982; Spanos *et al.* 1987) and the joint time-frequency analysis techniques have given rise to a number of stochastic simulation models based on time-frequency domain. A non-stationary analytical stochastic model for simulating earthquake accelerograms has been proposed by Conte and Peng (1997). The main idea of this model is to fit the analytical evolutionary power spectrum to the target power spectrum using least-square fitting method, in which the target power spectrum is determined from a single realization of random process by means of short-time multi-window (STMW) spectrum estimation method. Alternative ways to track the instantaneous time-frequency contents of a signal depend on the time-frequency analysis tools such as WT and EMD-HT, both identify time-dependent frequency information, thus offer different venues for the simulation of non-stationary random processes (e.g., Gurley and Kareem 1999; Iyama and Kuwamura 1999; Wen and Gu 2004; Wang and Kareem 2004[b]).

A new simulation method proposed in Wang and Kareem (2004[b]) for the simulation of non-stationary random processes is applied to the simulation of downburst wind field. The simulation procedure involves the wavelet and Hilbert transforms in tandem and relies on the ability of the SWT to decompose multi-component signal to mono-component signals that admits application the HT to derive instantaneous amplitude and frequency from the signal. By utilizing proper orthogonal decomposition of the covariance matrices of the instantaneous frequency, the simulation is extended to multivariate processes.

SIMULATION MODEL

In the numerical simulation of stationary random processes, typically independent uniformly distributed phase angles are employed in a Monte Carlo simulation scheme. In order to examine the distribution in case of a non-stationary signal, an example of data from a downburst shown in Fig. 4 is employed. Details of the data are discussed in the example. For the measured non-stationary downbust wind velocity, the distribution of its phase angles at each decomposition level may be regarded as still being approximately uniform, as presented in Fig. 5(b), but the phase differences do not exhibit a similar shape, as noted in Fig. 5(c). Several attempts have been reported in the literature to fit statistical distributions to the phase differences. Ohsaki (1979) has performed analysis on ground motion accelerograms and concluded that the probability distribution is "normal or normal-like" after introducing an appropriate shift of the phase difference to account for the asymmetry. Naraoka and Watanabe (1987) have employed a log-normal distribution for the phase differences to simulate accelerograms and Matsukawa *et al.* (1987) have fitted a normal distribution to the phase differences after a proper shift. After exploring the dependence of phase angle difference on Fourier amplitude, Thrainsson *et al.*(2000, 2002) propose beta distribution for large and intermediate Fourier amplitudes and the combination of beta and uniform distributions for small Fourier amplitudes.

Based on this wind data, an assumption of normal distribution is made in the proposed simulation model to fit instantaneous frequency as a random process at each frequency band. The examination of the instantaneous frequency distribution at each level of of the decomposed signal reveals dominant frequency component and similarity with the Gaussian distribution, with some departure in the tails, especially at lower levels such as the first level. To better represent the frequency information, such departure is excluded in a truncated Gaussian distribution. Therefore, the frequency falls into the range $[\mu_i - CL_i * \sigma_i, \mu_i + CR_i * \sigma_i]$ is taken as valid frequency fv_i and further formulate the mean and variance of Gaussian distribution, in which μ_i and σ_i denote the mean value and the standard deviation of the original frequency in each frequency band, respectively, and CL_i, CR_i are two constants at level i that define the boundary of the valid frequency, allowing for the flexibility to choose a reasonable range of the valid frequency for individual processes and levels. Based on the statistical information of valid frequency, instantaneous frequency are produced at each level using Gaussian assumption. The choice of the constants CL_i and CR_i at each level depends on the shape of each measured frequency, and may vary from 0.5 to 1.2. Appropriate values of the two constants provides good agreement between the Gaussian function and the valid frequency. Such comparisons are demonstrated in Fig. 5(c), in which the bright line representing the Gaussian distribution function is plotted together with the histogram. A good match between the two is observed.

The aforementioned simulation procedure is extended to multivariate processes by the proper orthogonal decomposition of the covariance matrix of instantaneous frequency. For the sample record of the non-stationary vector processes, $\mathbf{X(t)} = [X_1(t), X_2(t), ..., X_N(t)]^T$, its SWT and Hilbert transforms are obtained in sequence to yield mono-component subprocesses, instantaneous phase/frequency and instantaneous amplitude. The instantaneous frequency vector is expressed in terms of the eigenvectors of its covariance matrix:

$$\hat{\omega}_{k,n}(t) = \sum_{m=1}^{M} \Psi_{k,m} b_m(t) \tag{14}$$

where M is an appropriately selected dominant mode number ($M < N$). Accordingly, the multi-variate random processes can be simulated as:

$$\hat{X}_n(t) = Re[\sum_{k=1}^{K} a_{k,n}(t) e^{i \int \hat{\omega}_{k,n}(t)dt}] \tag{15}$$

The covariance function of the process is expressed as:

$$K_{\hat{X}_p \hat{X}_q}(t_1 t_2) = E \sum_{n=1}^{N} \sum_{n=1}^{N} a_{np}(t_1) a_{nq}(t_2) cos[\int^{t_1} (\omega_{np}(t) - \mu_{np})dt + \int^{t_2} (\omega_{nq}(t) - \mu_{nq})dt] \tag{16}$$

EXAMPLES

To demonstrate the strength of the proposed simulation method, a set of wind data simultaneously recorded on June 04 2002 by the Department of Atmospheric Science of Texas Tech University was employed herein. Fig. 4(a) shows the wind speed data simultaneously recorded at the same height (10m) at a Wind Engineering Mobile Instrument Towers 3,4,5 and 6, which are 263m apart, during the passage of a downburst. Corresponding time-varying mean in Fig. 4(b) presents the rapid velocity change during the passage of the downburst. The wavelet decomposition of the data recorded at Tower No. 3 is shown in Fig. 5(a), in which the first six plots present the detail functions and the bottom plot shows the approximation function, which is taken as the time-varying mean in this study. A comparison of the phase angle distribution to the uniform distribution, and the instantaneous frequency and the Gaussian distribution are shown in Figs. 5(b) and (c). In Figs. 6(a) and (b), its time-varying characteristics are noted, with high energy concentration in the frequency range up to 0.05 Hz during the time between 600 to 800 second. Simulation of a set of data using the proposed method is shown in Fig. 4(c). The Hilbert spectrum and scalogram of the simulation shown in Figs. 6(d) and (e) clearly show that the time-varying characteristics of the measured data are captured and preserved in the simulation process. To further explore the relationship between each component, Figs. 6(c) and (f) present the measured and simulated cross-scalogram of downburst data recorded at Tower No. 3 and 6. Obviously, as for the time-varying correlation relationship, the simulation and record show a good agreement.

DISCUSSION AND CONCLUSION

An alternative approach for analyzing non-stationary wind speed time histories was presented here. The concept of decomposing wind speed into the sum of a deterministic time-varying mean wind speed plus a stationary fluctuating wind speed was realized by DWT and EMD, which helped to eliminate the limitations of the stationarity assumption implied in the traditional approach. Field measurement of wind data recorded during Hurricane Lili, 2002 was used to verify the proposed approach. The power spectral density of the fluctuating components obtained by DWT or EMD had lower amplitude in the low frequency range when compared to the traditional approach, while in the higher frequency range they were found to be very similar. This is due to the presence of low frequency trend in the wind fluctuations obtained traditionally, which is filtered out in the process of removing the time varying mean. Turbulence intensities obtained by the DWT and EMD were very close to those by the traditional approach with slightly reduced values. Intuitively, the results were more realistic as the constant mean process should yield higher intensity, which is rather unrealistic. The gust factors obtained by the DWT and EMD are similar to those obtained by the traditional approach. It can be concluded that the concept of time-varying mean wind speed can be applied in the analysis of wind speed data through the application of DWT or EMD. From the above observations, it was concluded that while processing hurricane data, time-varying mean was a more realistic quantity for separating the original signal into two categories than the constant hourly mean. It represented the trend of the wind speed, and the remaining fluctuating component complied with the Gaussian assumption. The proposed approach has the merit of becoming a method of choice for engineering applications in the near future.

A dual-domain, i.e., time and frequency, method to examine the evolutionary characteristics of a downburst wind speed was presented. By invoking both SWT and HT in tandem, it was shown that the instantaneous frequency at different decomposition levels followed a distribution close to Gaussian. Based on the observation, the assumption of instantaneous frequency following Gaussian distribution was introduced to facilitate the simulation of downburst wind speed. Numerical examples concerning the simulation of actual downburst simultaneously recorded at the same height and horizontally apart demonstrated the efficacy of the simulation scheme, which resulted in a simulation that captured the time-varying characteristics of the measured data and preserved the correlation between components. The proposed description and simulation of the downburst data facilitated better understanding of the phenomena and showed the potential of effectively simulating downburst related wind loads on structures.

ACKNOWLEDGMENTS

The support for this work was provided in part by the NSF Grant CMS03-24331.

References

[1] C. H. Yeh, and Y. K. Wen (1990), "Modeling of nonstationary ground motion and analysis of inelastic structural response", *Struct. Safety*, 8(1-4), 281-298.

[2] J. P. Conte (1992), "Effects of earthquake frequency nonstationarity on inelastic structural response", *Proc. 10th World Conf. on Earthquake Engrg.*, A. A. Balkema, Rotterdam, The Netherlands.

[3] J. Ashcroft (1994), "The relationship between the gust ratio, terrain roughness, gust duration and the hourly mean wind speed", *Journal of Wind Engineering and Industrial Aerodynamics*, 53(3), 331-355.

[4] A. D. Smith, C. K. Mehta (1993), "Investigation of stationary and nonstationary wind data using classical Box-Jenkins models", *Journal of Wind Engineering and Industrial Aerodynamics*, 49(1-3), 319-328.

[5] K. Gurley, A. Kareem (1999), "Applications of wavelet transforms in earthquake, wind and ocean engineering," *Engineering Structures*, v. 21, p. 149-167.

[6] J. Chen, Y. L. Xu (2004), "On modeling of typhoon-induced non-stationary wind speed for tall buildings", *The Structural Design of Tall and Special Buildings*, 13, 145-163.

[7] L. Wang, A. Kareem (2004^a),"Modeling of Non-Stationary Winds in Gust-Fronts", ASCE Joint Specialty Conference on Probabilistic Mechanics and Structural Reliability, Albuquerque, New Mexico, July 26-28.

[8] T. T. Fujita (1985), Report of Projects NIMROD and JAWS, University of Chicago.

[9] J. McCarthy, T. T. Fujita (1982), "The Joint Airport Weather Studies Project", *Bulletin of American Meteorology Society*, 63, 15-22.

[10] J. D. Holmes, S. E. Oliver (2000), "An empirical model of a downburst", *Engineering Structures*, 22, 1167-1172.

[11] R. M. Oseguera, R. L. Bowles (1988), "A simple analytic 3-dimensional downburst model based on boundary layer stagnation flow", NASA Technical Memorandum 100632.

[12] D. D. Vicroy (1992), "Assessment of microburst models for downdraft estimation", *Journal of Aircraft*, 29, 1043-1048.

[13] G. S. Wood, K. C. S. Kwok, N. A. Motteram, and D. F. Fletcher (2001), "Physical and numerical modeling of thunderstorm downbursts", *Journal of Wind Engineering and Industrial Aerodynamics*, 89(6), 535-552.

[14] L. Chen, C. W. Letchford (2004), "A deterministic-stochastic hybrid model of downbursts and its impact on a cantilevered structure", *Engineering Structures*, 26, 619-629.

[15] L. Chen, C. W. Letchford (2005), "Proper orthogonal decomposition of two vertical profiles of full-scale non-stationary downburst wind speeds", *Journal of Wind Engineering and Industrial Aerodynamics*, 93, 187-216.

[16] A. Kareem, T. Kijewski (2002), "Time-frequency analysis of wind effects on structures", *Journal of Wind Engineering and Industrial Aerodynamics*, 90 (12-15), 1435-1452.

[17] T. Kijewski, A. Kareem (2003), "Wavelet transform for system identification in civil engineering", *Computer Aided Civil and Infrastructure Engineering*, 18, 339-355.

[18] D. B. Percival, A. T. Walden (2000), *Wavelet Methods for Time Series Analysis*, Cambridge University Press.

[19] N. E. Huang, Z. Shen, S. R. Long, M. L. Wu, H. H. Shih, Q. Zheng, N. C. Yen, C. C. Tung, and H. H. Liu (1998), "The empirical mode decomposition and the Hilbert spectrum for nonlinear and non-stationary time series analysis " *Proceedings of Royal Society. Lond. A* , vol.454, 903-995.

[20] T. Kijewski-Correa, A. Kareem (2004), "Time-frequency characterization of nonlinear dynamical systems", 9^{th}*ASCE Joint Specialty Conference on Probabilistic Mechanics and Structural Reliability*.

[21] S. Olhede, A. T. Walden (2004), "The Hilbert spectrum via wavelet projections", *Proc. R. Soc. Lond. A*, 460, 955-975.

[22] K. Gurley(2002), Personal Communication.

[23] G. Deodatis, M. Shinozuka (1988), "Auto-regressive model for nonstationary stochastic processes", *Journal of Engineering Mechanics*, 114(11), 1995-2012.

[24] Y. Li, A. Kareem (1991), "Simulation of multivariate non-stationary random processes by FFT" *Journal of Engineering Mechanics*, vol.117, No.5, 1037-1058.

[25] R. J. Scherer, J. D. Riera, and G. I. Schueller (1982), "Estimation of the time-dependent frequency content of earthquake accelerations", *Nuclear Engrg. and Des.*, 71(3), 301-310.

[26] P. Spanos, J. Roesset, and M. Donley (1987), “Evolutionary power spectrum estimation of September 19, 1995 Mexico Earthquake accelerograms”, *Stochastic Approaches in Earthquake Engrg., Proc., U.S.-Japan Joint Seminar*, Y. K. Lin and R. Minai, eds., Springer-Verlag, New York, N. Y.

[27] J. P. Conte, B. F. Peng (1997), “Fully nonstationary analytical earthquake ground-motion model”, *Journal of Engineering Mechanics*, 123(1), 15-24.

[28] J. Iyama, H. Kuwamura (1999), “Application of wavelets to analysis and simulation of earthquake motions”, *Earthquake Engineering and Structural Dynamics*, 28, 255-272.

[29] Y. K. Wen, P. Gu (2004), “Description and simulation of nonstationary processes based on Hilbert spectra”, *Journal of Engineering Mechanics, ASCE*, 130(8).

[30] L. Wang, A. Kareem (2004^b), “Simulation of Non-Stationary Random Processes: A Wavelet and Hilbert Transforms Perspective”, ASCE Joint Specialty Conference on Probabilistic Mechanics and Structural Reliability, Albuquerque, New Mexico, July 26-28.

[31] Y. Ohsaki (1979), “On the significance of phase content in earthquake ground motions”, *Journal of Engineering and Structural Dynamics*, 7, 427-439.

[32] K. Naraoka, T. Watanabe (1987), “Generation of nonstationary earthquake ground motions using phase characteristics”, *Trans. of the 9^{th} Inter. Conf. on Struct. Mech. in Reactor Tech.*, vol. K1, 49-54.

[33] K. Matsukawa, T. Watanabe, N. A. Theofanopulos, and M. Tohdo (1987), “Phase characteristics of earthquake ground motions and those applications to synthetic ones”, *Trans. of the 9^{th} Inter. Conf. on Struct. Mech. in Reactor Tech.*, vol. K1, 43-48.

[34] H. Thrainsson, A. S. Kiremidjian, and S. R. Winterstein (2000), “Modeling of earthquake ground motion in the frequency domain”, *John A. Blume Earthquake Engineering Center Report No. 134*, Dept. of Civil and Environmental Engineering, Stanford University, Stanford, CA.

[35] H. Thrainsson, A. S. Kiremidjian (2002), “Simulation of digital earthquake accelerograms using the inverse discrete Fourier transform”, *Earthquake Engineering and Structural Dynamics*, 31(12), 2023-2048.

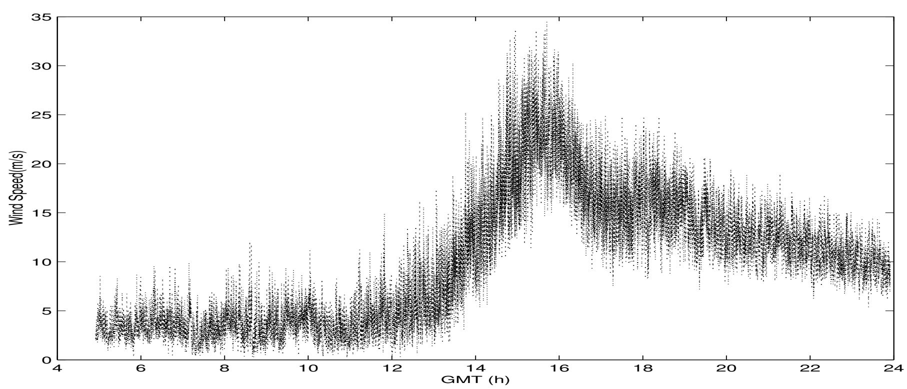

Fig. 1 Wind Speed Time History

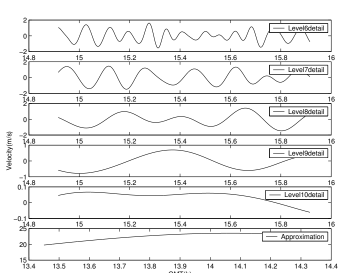

a) DWT

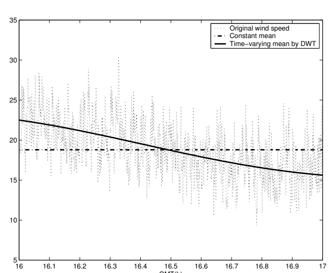

b) Mean Comparison

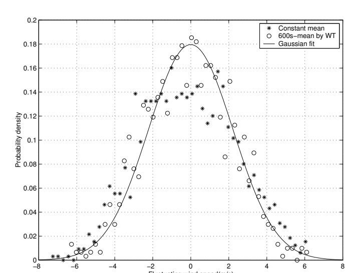

c) pdf

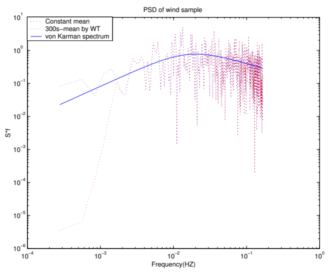

d) psd

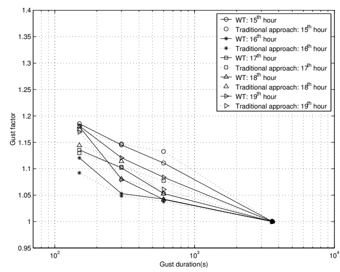

e) Gust Factor

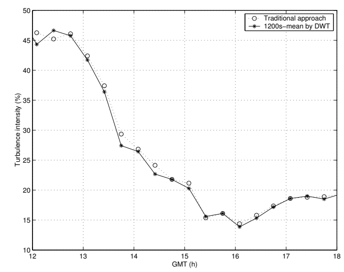

f) Turbulence Intensity

Fig. 2. Analysis based on Discrete Wavelet Decomposition

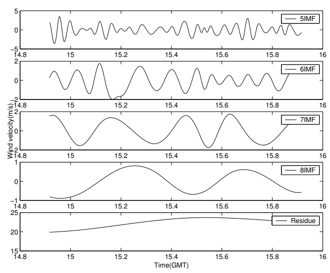

a) EMD

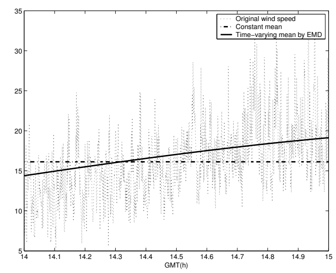

b) Mean Comparison

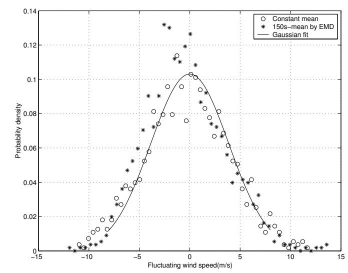

c) pdf

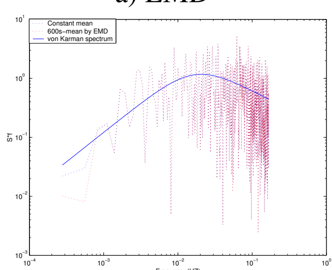

d) psd

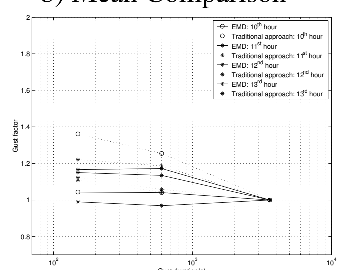

e) Gust Factor

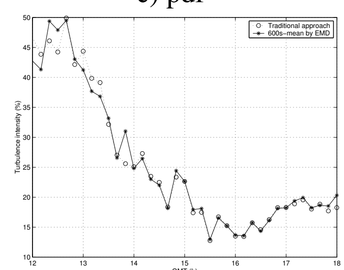

f) Turbulence Intensity

Fig. 3. Analysis based on Empirical Mode Decomposition

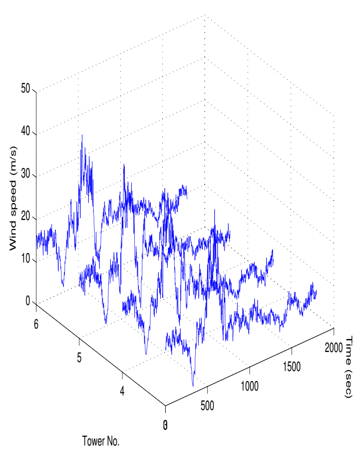

a) Measurements

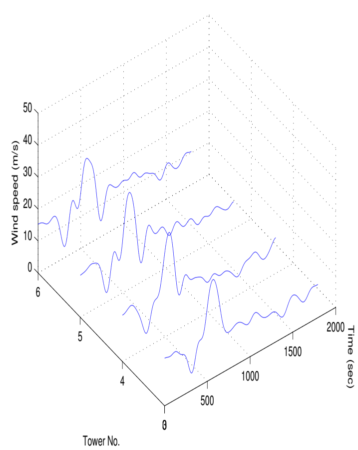

b) Time-dependent means

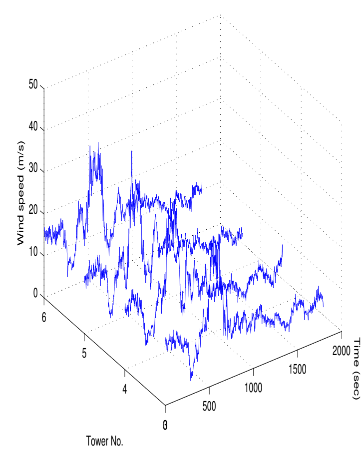

c) Simulations

Fig. 4. Downburst data 263m apart

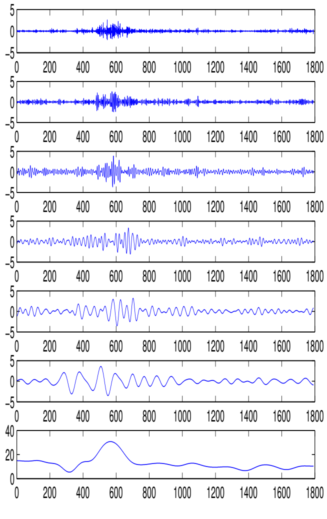

a) Decomposition

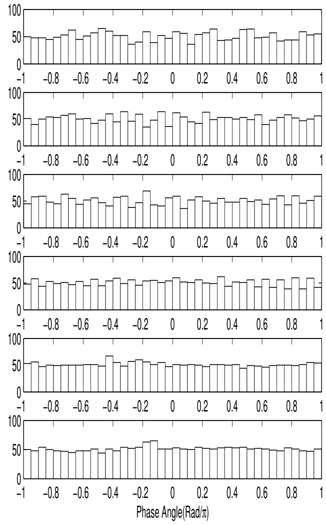

b) Phase angles

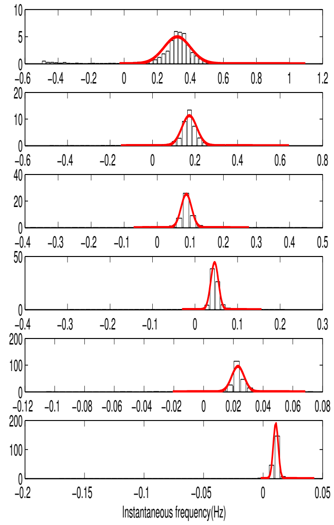

c) Instantaneous frequency

Fig. 5. Downburst data at height 6m

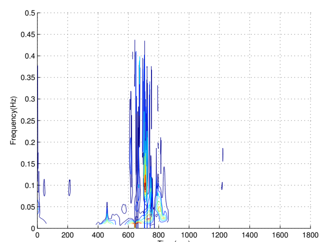

a) Hilbert Spectrum

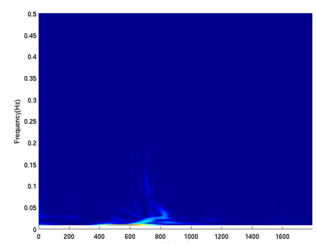

b) Scalogram

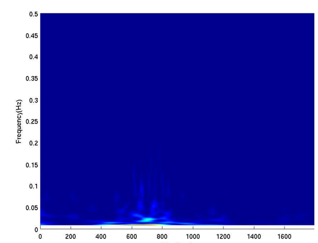

c) Cross Scalogram

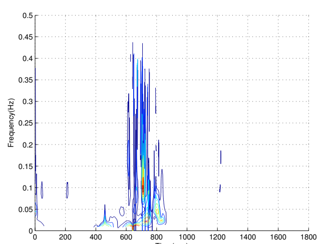

d) Hilbert Spectrum

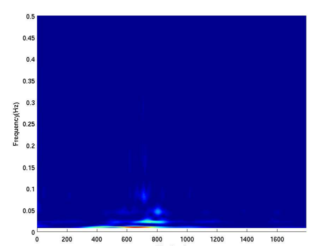

e) Scalogram

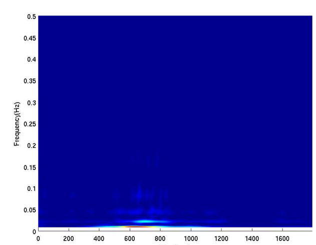

f) Cross Scalogram

Fig. 6. Comparison of Simulated and Measured Data